Free Surface Flow Simulation Using Moving-Grid Finite-Volume Method

*Sadanori Ishihara¹, †Kenichi Matsuno², †Masashi Yamakawa², †Takeshi Inotomo¹, and †Shinichi Asao³

¹Graduate School of Science and Technology, Kyoto Institute of Technology, Matsugasaki, Sakyo-ku, Kyoto, Japan ²Department of Mechanical System Engineering, Kyoto Institute of Technology, Matsugasaki, Sakyo-ku, Kyoto, Japan. ³Department of Mechanical Engineering, College of Industrial Technology, 1-27-1, Nishikoya, Amagasaki, Hyogo, Japan.

*Presenting author: d4821001@edu.kit.ac.jp †Corresponding author: d4821001@edu.kit.ac.jp

Abstract

In this paper, an interface-tracking method combined with the Moving-Grid Finite-Volume method is presented for simulating free surface flows. In the interface-tracking method, the calculation grid is moved and deformed according to the movement of the free surface. For tracking free surface, surface height equation for the free surface shape was solved. We applied this method to some flow cases with free surface. Numerical results show that the present new flows simulation method using Moving-Grid Finite-Volume method is very accurate and have a promising feature for free surface flows.

Keywords: Free Surface Flows, Computational Fluid Dynamics, Moving-Grid, Finite Volume Method

Introduction

Free surface flows are important from a point of view of engineering. For example, sloshing flow in tanks, mixing in vessels, jet from nozzle and injection molding are free surface flows.

Many numerical methods are presented for free surface flows [Scardovelli and Zaleski (1999)].

These method can be classified to two approaches, interface-capturing method and interface-tracking method.

In the interface-capturing method, fixed grid is used. For free surface capturing, particle movement or some function is solved. MAC method [Harlow and Welch (1965)], VOF method [Hirt and Nichols (1981)] and level set method [Sussman at al. (1994)]) are used in this approach. These method can solve bubble flow and breaking waves. However, these method often have interface smearing.

On the other hand, in the interface-tracking method, moving grid is used. For free surface tracking, computational grids are moved and deformed according to movement of free surface. ALE [Okamoto and Kawahara (1990); Lo and Young (2004); Ushijima (1998)] and Finite Volume method [Apsley and Hu (2003); Muzaferija and Peric (1997)] are used in this approach. This approach is very simple and can track free surface with sharp interface. However, computational grids are usually large deformed.

Free surface flow can be interpreted as a moving boundary problem. For moving boundary problems, Moving-Grid Finite-Volume Method was suggested [Mihara and (1999)]. This method can solve flow with moving grids with satisfying physical and geometrical conservation laws. The method has been applied to various flows [Mihara et al. (1999); Watanabe and Matsuno (2009); Matsuno (2010)]. However, these applications have been limited to single phase flows.

The purpose of this paper is to extend the Moving-Grid Finite-Volume Method to free surface flows. The main advantages of this method is simple treatment with free surface and satisfying physical and geometrical conservation laws.

In some test cases with free surface, comparison with analytical solution or experimental data are presented.

Governing Equations

The governing equations are the continuity equation and the nondimensionalized incompressible Navier-Stokes equations. These equation are written as follows:

$$\frac{\partial u}{\partial x} + \frac{\partial v}{\partial y} + \frac{\partial w}{\partial z} = 0, \tag{1}$$

and

$$\frac{\partial \mathbf{q}}{\partial t} + \frac{\partial \mathbf{E}}{\partial x} + \frac{\partial \mathbf{F}}{\partial y} + \frac{\partial \mathbf{G}}{\partial z} = \mathbf{H} , \qquad (2)$$

where x, y and z are coordinates, t is time. u, v and w are velocities in x, y and z directions, respectively. q is the velocity vector, $q = [u, v, w]^T$. E, F and G are flux vectors in x, y and z directions, respectively. H is the body force term including gravity. Flux vectors are written as follows:

$$\boldsymbol{E} = \hat{\boldsymbol{E}} - \boldsymbol{E}_{v} + \boldsymbol{E}_{p}, \, \boldsymbol{F} = \boldsymbol{F} - \boldsymbol{F}_{v} + \boldsymbol{F}_{p}, \, \boldsymbol{G} = \hat{\boldsymbol{G}} - \boldsymbol{G}_{v} + \boldsymbol{G}_{p},$$
(3)

where \hat{E}, \hat{F} and \hat{G} are the advection flux vectors, E_v, F_v and G_v are the viscous flux vectors, and E_p, F_p and G_p are pressure flux vectors in x, y and z directions, respectively. The elements of flux vectors and body force term are:

$$\boldsymbol{E} = \begin{bmatrix} u^{2} \\ uv \\ uw \end{bmatrix}, \boldsymbol{F} = \begin{bmatrix} vu \\ v^{2} \\ vw \end{bmatrix}, \boldsymbol{G} = \begin{bmatrix} wu \\ wv \\ w^{2} \end{bmatrix}, \boldsymbol{E}_{v} = \frac{1}{\text{Re}} \begin{bmatrix} u_{x} \\ v_{x} \\ w_{x} \end{bmatrix}, \boldsymbol{F}_{v} = \frac{1}{\text{Re}} \begin{bmatrix} u_{y} \\ v_{y} \\ w_{y} \end{bmatrix}, \boldsymbol{G}_{v} = \frac{1}{\text{Re}} \begin{bmatrix} u_{z} \\ v_{z} \\ w_{z} \end{bmatrix},$$

$$\boldsymbol{E}_{p} = \begin{bmatrix} p \\ 0 \\ 0 \end{bmatrix}, \boldsymbol{F}_{p} = \begin{bmatrix} 0 \\ p \\ 0 \end{bmatrix}, \boldsymbol{G}_{p} = \begin{bmatrix} 0 \\ 0 \\ p \end{bmatrix}, \boldsymbol{H} = \begin{bmatrix} X \\ 0 \\ -\frac{1}{\text{Fr}^{2}} \end{bmatrix}, \tag{4}$$

where p is the pressure, Re is the Reynolds number and Fr is the Froude number. The subscripts x, y and z indicate derivatives with respect to x, y and z respectively. X is the body force in x direction. Reynolds number and Froude number are:

Re =
$$\frac{\overline{U}_0 \overline{L}_0}{\overline{v}}$$
, Fr = $\frac{\overline{U}_0}{\sqrt{\overline{g}\overline{L}_0}}$, (5)

where \overline{L}_0 is the characteristics length, \overline{U}_0 is the characteristics velocity, \overline{v} is the kinematic viscosity and \overline{g} is the gravitational acceleration. Over bar shows the dimensional quality.

Discretization method and numerical method

Discretization method

In discretization for these equations, we use Moving-Grid Finite-Volume Method. This discretization method is based on cell-centered Finite-Volume Method in space-time unified

domain. In three-dimensional case, four-dimensional polyhedron in the (x, y, z, t) control volume is used.

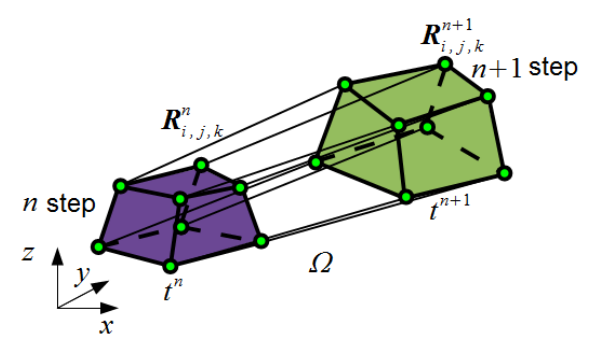


Figure 1. Schematic drawing of control volume

Fig. 1 shows schematic drawing of structured control volume in (x, y, z, t) unified domain. \mathbf{R} is grid position vector, $\mathbf{R} = [x, y, z]^T$, where superscript n shows time step and subscript i, j, k show structured grid point indexes. The purple region is n time step computational cell, green region is n+1 step computational cell. The control volume is four-dimensional polyhedron Ω . Eq. (2) is integrated with the control volume Ω as

$$\int_{\Omega} \left(\frac{\partial \mathbf{q}}{\partial t} + \frac{\partial \mathbf{E}}{\partial x} + \frac{\partial \mathbf{F}}{\partial y} + \frac{\partial \mathbf{G}}{\partial z} \right) d\Omega = V_{\Omega} \mathbf{H} , \qquad (6)$$

where V_{Ω} is a four-dimensional volume $(V_{\Omega} = \int_{\Omega} d\Omega)$. Eq. (6) is divergence form in (x, y, z, t)

dimension. By using Gaussian divergence theorem, Eq. (6) is written as,

$$\int_{\Omega} \left[\left(\frac{\partial}{\partial x}, \frac{\partial}{\partial y}, \frac{\partial}{\partial z}, \frac{\partial}{\partial t} \right) \cdot (E, F, G, q) \right] d\Omega = \oint_{\partial \Omega} \left[(E, F, G, q) \cdot n \right] d(\partial \Omega) = V_{\Omega} H,$$
(7)

where n is the vector normal to control volume surface. $\partial \Omega$ is the surface of the control volume. The n_x, n_y, n_z and n_t are components of n in x, y, z and t directions, respectively. From Eq. (7), we can write as,

$$\sum_{t=1}^{8} (q n_t + \boldsymbol{\Phi} - \boldsymbol{\Psi} + \boldsymbol{\Pi}) = V_{\Omega} \boldsymbol{H}, \qquad (8)$$

where,

$$\boldsymbol{\Phi} = \hat{\boldsymbol{E}} n_x + \hat{\boldsymbol{F}} n_y + \hat{\boldsymbol{G}} n_z, \, \boldsymbol{\Phi} = \frac{1}{\text{Re}} \left(\boldsymbol{E}_v n_x + \boldsymbol{F}_v n_y + \boldsymbol{G}_v n_z \right), \, \boldsymbol{\Pi} = \boldsymbol{E}_p n_x + \boldsymbol{F}_p n_y + \boldsymbol{G}_p n_z.$$
(9)

The subscript l in Eq. (8) denotes the surface of the control volume in four dimension (x, y, z, t). The l = 7 surface normal vector is the computational cell at n time step, l = 8 surface normal vector is the computational cell at n + 1 time step. For example, Fig. 2 shows the control volume surface at l = 2.

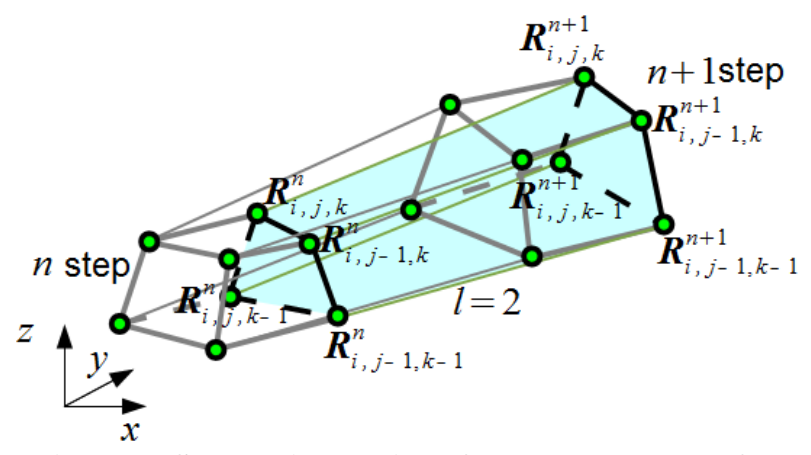


Figure 2. Schematic drawing of control volume surface

Control volume surfaces at l = 7, l = 8 are perpendicular to the t axis. Eq. (8) becomes as follows:

$$\boldsymbol{q}^{n+1} (n_t)_8 + \boldsymbol{q}^n (n_t)_7 + \sum_{t=1}^6 (\boldsymbol{q}^{n+1/2} n_t + \boldsymbol{\Phi}^{n+1/2} - \boldsymbol{\Psi}^{n+1/2} + \boldsymbol{\Pi}^{n+1/2}) = V_{\Omega} \boldsymbol{H} . \tag{10}$$

This Eq. (10) is discretized equation.

Numerical method

To solve Eq. (10), we use SMAC method [Amsden and Harlow (1970)]. Intermediate velocity is solved iteratively using LU-SGS method [Yoon and Jameson (1988)]. The inviscid term Φ and moving grid term qn_t are evaluated using QUICK method [Leonard (1979)]. The viscid term Ψ and pressure gradient term Π are evaluated using central difference scheme. The Poisson equation about pressure correction is solved iteratively using Bi-CGSTAB [van der Vorst (1992)].

Interface-Tracking method

In present method, a surface height equation [Apsley and Hu (2003)] is solved for free surface height. Fig. 3 shows free surface shape.

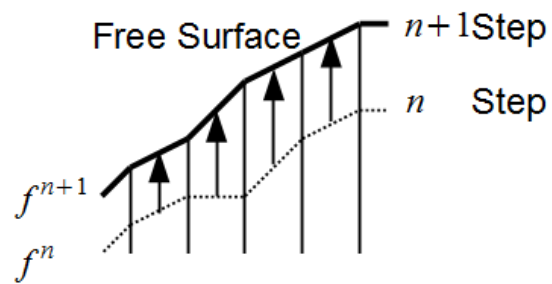


Figure 3. Free surface height

In Fig. 3, f = f(x, y, t) is the surface height function. The surface height equation is as follows:

$$\frac{\partial f}{\partial t} + u \frac{\partial f}{\partial x} + v \frac{\partial f}{\partial y} = w. \tag{11}$$

Eq. (11) can be discretized as follows:

$$f_{i,j}^{n+1} = f_{i,j}^{n} - \Delta t \left(u f_{x} + v f_{y} - w \right)^{n}, \tag{12}$$

where Δt is time step size, superscript n shows time step and subscript i, j, k shows grid point indexes. The uf_x and vf_y in Eq. (12) are evaluated using 1st order upwind differencing scheme. Once the free surface height is solved, computational grids moved and deformed according to the movement of the free surface. In the present study, the surface tension is neglected. The pressure on the free surface is fixed by p = 0.

Numerical Results

Sloshing flow case

To check the present method, sloshing flow case is solved. A comparison was made with the experimental result [Okamoto and Kawahara (1990)]. The geometry of the domain is shown in Fig. 4.

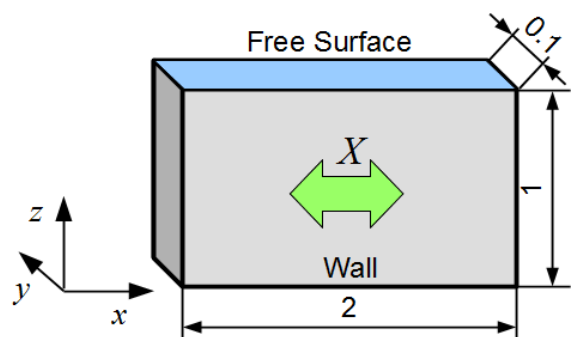


Figure 4. Geometry of sloshing flow case

The size of the initial domain is $2 \times 0.1 \times 1$. The calculation domain is nondimensionalized by initial free surface height.

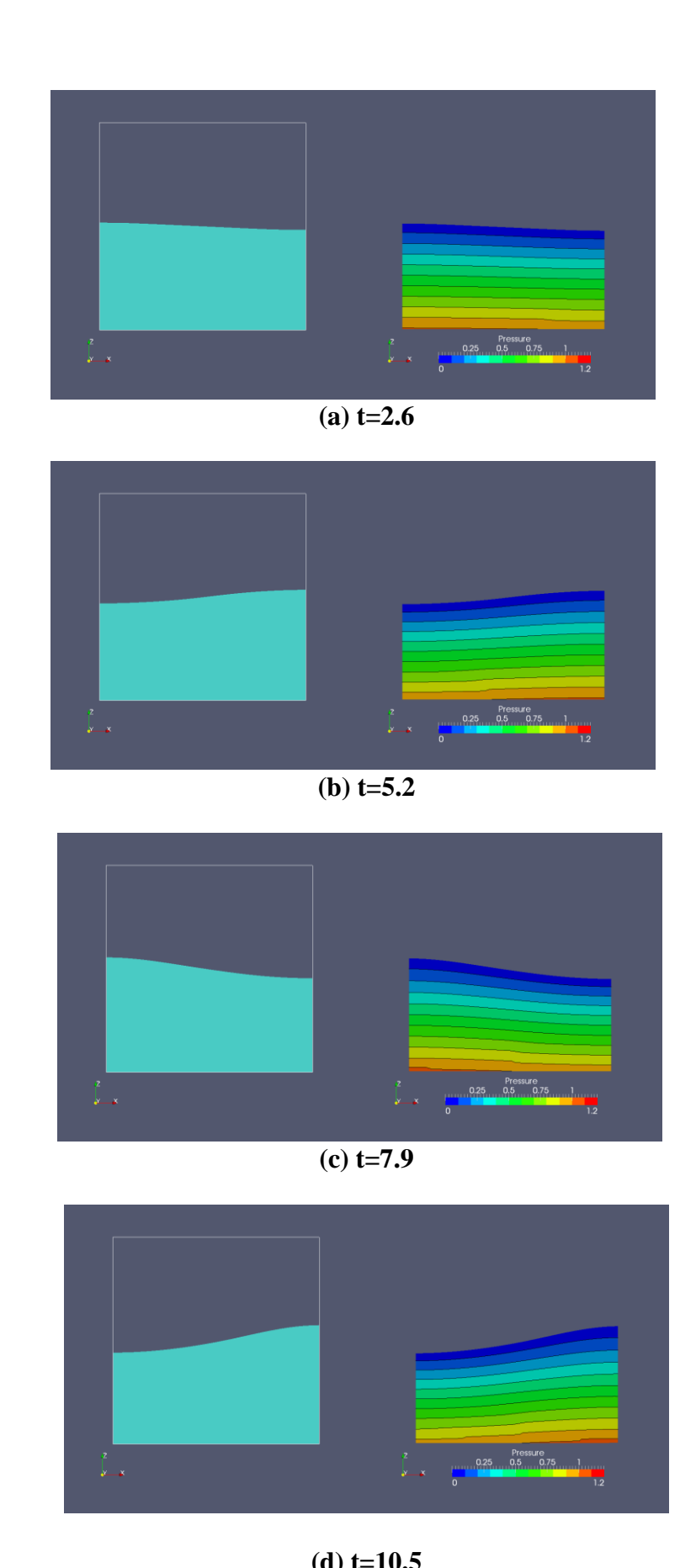
In our case, fluid flow with oscillating body force is solved. The body force is as follows:

$$X = -A\varpi^2 \sin \varpi t \,, \tag{13}$$

where A = 0.00186 and $\varpi = 1.20$ are the amplitude and frequency of the oscillation, respectively. The numerical grid used for calculation had $61 \times 11 \times 51$ grid points. The time step size is 0.001. The Reynolds number is 1.1×10^6 and the Froude number is 1.

The initial condition of the velocity is given by u = v = w = 0. The initial condition of the pressure is given by p = 0. The boundary conditions is as follows. In the wall boundary, the velocity is slip condition and the pressure is Neumann boundary condition. In the free surface, the velocity is 0th extrapolated and the pressure is fixed by p = 0.

Fig. 5 shows numerical simulation results. In these figures, the left column show the free surface shape and the right column show pressure distributions at t=2.6, 5.2, 7.9 and 10.5. From the free surface shape, nonlinear surface movement is appeared.



 $\label{eq:continuous} (d)~t{=}10.5$ Figure 5. Results of sloshing flow case (left : surface shape, right : pressure distributions)

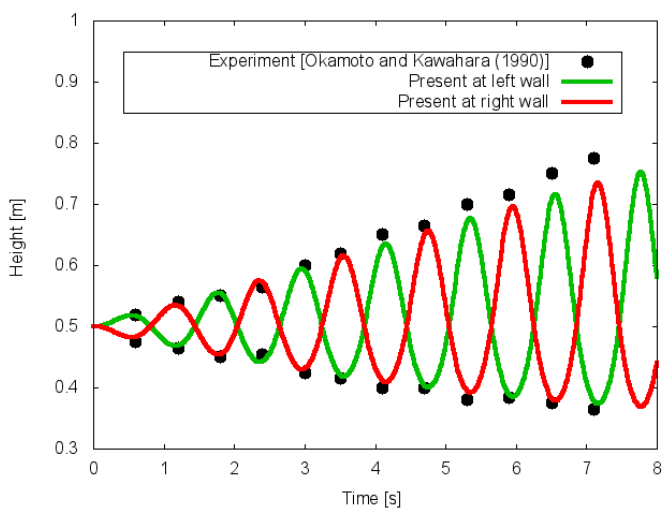
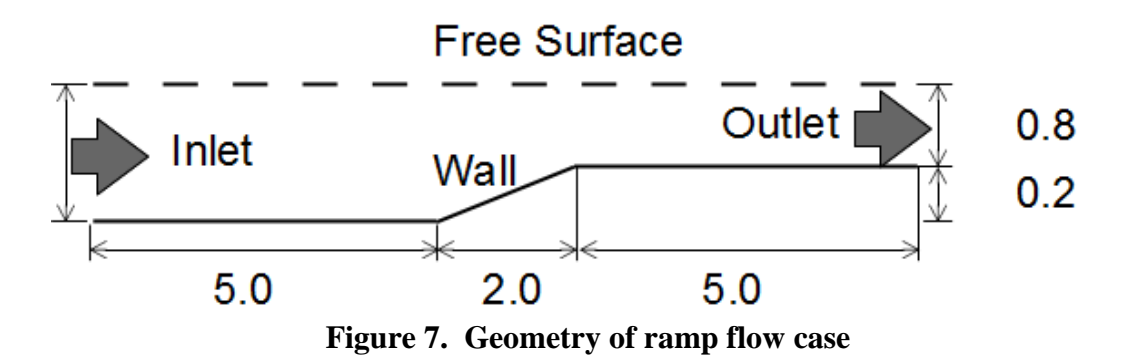


Figure 6. Time history of the free surface elevation at the left wall and the right wall

Fig. 6 shows the time history of the free surface elevation at the left wall and right wall. The initial free surface height is 0.5 m. Points are experimental results [Okamoto and Kawahara (1990)], green lines is present result at the left wall and red line is present result at the right wall. As shown in Fig. 6, surface height at the left wall and the right wall increase alternately, and present results agree reasonably with experimental one. From these results, the present method can apply sloshing analysis.

Ramp flow case

In inviscid case, flow over a ramp [Apsley and Hu (2003); Muzaferija and Peric (1997)] is solved. This case is basic test case with free surface flow. The geometry of the domain is shown in Fig. 7. Four Froude number condition cases were solved: subcritical flow at Fr=0.3, 0.32 and supercritical flow at Fr=1.92, 2. These conditions are same as references Fr=0.3, 2.0 [Apsley and Hu (2003)] and Fr=0.32, 1.92 [Muzaferija and Peric (1997)].



The calculation domain is nondimensionalized by initial free surface height. The numerical grid used for calculation had $61 \times 11 \times 31$ grid points. The time step size is 0.005. In this case, inviscid flow is assumed. The Froude number is 0.3, 0.32, 1.92 and 2.0.

The initial condition of velocity is given by u = 1, v = w = 0. The initial condition of pressure is given by hydrostatic pressure. The boundary conditions as follows. In the inlet boundary, the velocity is fixed by u = 1, v = w = 0, and the pressure is Neumann boundary condition. In the outlet boundary, the velocity is 0th extrapolated and the pressure is 0th extrapolated. In the bottom wall boundary, the velocity is slip condition and the pressure is Neumann boundary condition. In the

front and back boundary, the velocity is slip condition and the pressure is Neumann boundary condition. In the free surface, the velocity is 0th extrapolated and the pressure is fixed by p = 0. Fig. 8 shows the free surface shape of Fr=0.3 case at t=200. Fig. 9 shows the free surface shape of Fr=2.0 case at t=200.

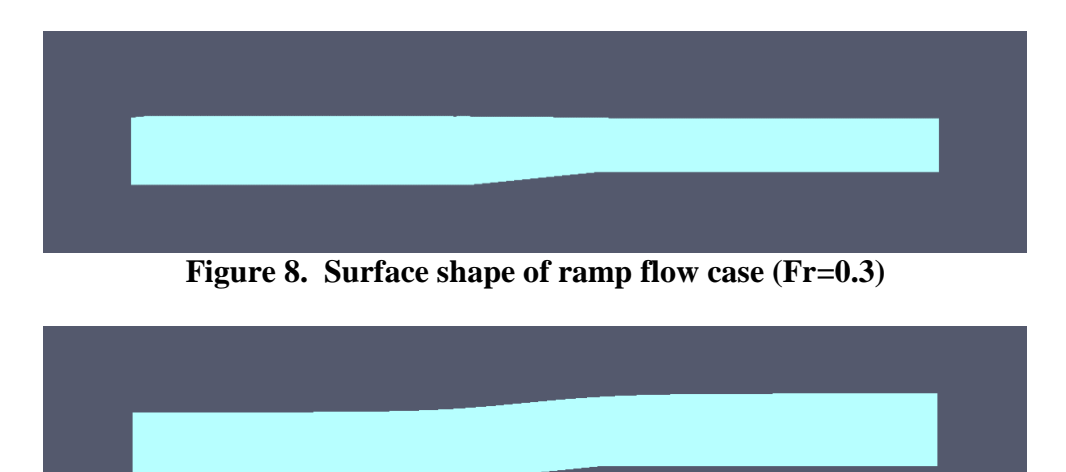


Figure 9. Surface shape of ramp flow case (Fr=2.0)

As shown in Fig. 8, the free surface height at the outlet boundary decrease from the inlet boundary. On the other hand, as shown in Fig. 9, the free surface height at the outlet boundary increase from the inlet boundary. These results are caused by subcritical (Fr=0.3) or supercritical (Fr=2.0) conditions.

Table 1 shows the free surface height from the bottom wall at the outlet boundary. In Table 1, 1-d theory shows analytical results using 1-d theory [Apsley and Hu (2003)]. Present shows present results. Error shows our results error from 1-d theory. As shown in Table 1, our results are agree with reference solutions and 1-d theory solutions.

		Froude number		
	0.3	0.32	1.92	2
1-d theory	0.7689	0.7635	1.0897	1.0776
Present	0.7949	0.7940	1.0910	1.0794
Error [%]	3.39	3.98	0.12	0.17
Apsley and Hu (2003)	0.7687			1.0792
Muzaferija and Peric (1997)		0.7752	1.0992	

Table 1. Free surface height of ramp flow case

Conclusions

In this paper, new flow simulation method with free surface is presented. This method is based on the Moving-Grid Finite-Volume Method and coupled with the interface-tracking method. We applied present new method to some flow cases. From the comparison with experimental or numerical data, present method using the Moving-Grid Finite-Volume method is very accurate and have a promising feature for free surface flows.

Acknowledgment

This work was supported by JSPS KAKENHI Grant Numbers 24560192, 25420120.

References

- Amsden, A. A. and Harlow, F. H. (1970) A simplified MAC technique for incompressible fluid flow calculations, *Journal of Computational Physics* **6**-2, 322–325.
- Apsley, D. and Hu, W. (2003) CFD simulation of two- and three-dimensional free-surface flow, *International Journal* for Numerical Methods in Fluids **42**, 465–491.
- Harlow, F. H. and Welch, J. E. (1965) Numerical calculation of time-dependent viscous incompressible flow of fluid with free surface, *The Physics of Fluids*, **8**-12, 2182–2189.
- Hirt, C. W. and Nichols, B. D. (1981) Volume of fluid (VOF) method for the dynamics of free boundaries, *Journal of Computational Physics* **39**-1, 201–205.
- Scardovelli, R. and Zaleski, S. (1999) Direct numerical simulation of free surface and interfacial flow, *Annual Review of Fluid Mechanics* **31**, 561–603.
- Sussman, M., Smereca, P. and Osher, S. (1994) A level set approach for computing solutions for incompressible two-phase flow, *Journal of Computational Physics* **114**-1, 146–159.
- Leonard, B. P. (1979) A stable and accurate convective modeling procedure based on quadratic interpolation, *Computer Methods in Applied Mechanics and Engineering* **19**, 59–98.
- Lo, D. C. and Young, D. L. (2004) Arbitary Lagrangian-Eulerian finite element analysis of free surface flow using a velocity-vorticity formulation, *Journal of Computational Physics* **195**-1, 175–201.
- Matsuno, K. (2010) Development and applications of a moving grid finite volume method, in developments and applications in engineering computational technology, Chapter 5, ed. Topping, B. H. V. et al., *Saxe-Coburg Publications*, 103–129.
- Mihara, K., Matsuno, K. and Satofuka, N. (1999) An iterative finite-volume scheme on a moving grid (1st report, the fundamental formulation and validation), *Transactions of the Japan Society of Mechanical Engineers Series B* **65**-637, 2945–2953 (in Japanese).
- Muzaferija, S. and Peric, M. (1997) Computation of free-surface flows using the finite-volume method and moving grids, *Numerical Heat Transfer Part B* **32**, 360–384.
- Okamoto, T. and Kawahara, T. (1990) Two-dimensional sloshing analysis by Lagrangian finite element method, *International Journal for Numerical Methods in Fluids* 11, 453–477.
- Ushijima, S. (1998) Three –dimensional arbitrary Lagrangian-Eulerian numerical prediction method for non-linear free surface oscillation, *International Journal for Numerical Method in Fluids* **26**, 605–623.
- van Der Vorst, H. (1992) Bi-CGSTAB: A fast and smoothly converging variant of Bi-CG for the solution of nonsymmetric linear Systems, *SIAM Journal on Scientific Computing* **13**-2, 631–644.
- Watanabe, K. and Matsuno, K. (2009) Moving computational domain method and its application to flow around a high-speed car passing through a hairpin curve, *Journal of Computational Science and Technology* **3**, 449–459.
- Yoon, S. and Jameson, Y. (1988) Lower-upper symmetric-Gauss-Seidel methods for the Euler and Navier-Stokes equations, *AIAA Journal* **26**, 1025–1026.